Precision Range Image Registration Using a Robust Surface Interpenetration Measure and Enhanced Genetic Algorithms

Luciano Silva, *Member*, *IEEE*, Olga R.P. Bellon, *Member*, *IEEE*, and Kim L. Boyer, *Fellow*, *IEEE*

Abstract—This paper addresses the range image registration problem for views having low overlap and which may include substantial noise. The current state of the art in range image registration is best represented by the well-known iterative closest point (ICP) algorithm and numerous variations on it. Although this method is effective in many domains, it nevertheless suffers from two key limitations: It requires prealignment of the range surfaces to a reasonable starting point and it is not robust to outliers arising either from noise or low surface overlap. This paper proposes a new approach that avoids these problems. To that end, there are two key, novel contributions in this work: a new, hybrid genetic algorithm (GA) technique, including hillclimbing and parallel-migration, combined with a new, robust evaluation metric based on surface interpenetration. Up to now, interpenetration has been evaluated only qualitatively; we define the first quantitative measure for it. Because they search in a space of transformations, GAs are capable of registering surfaces even when there is low overlap between them and without need for prealignment. The novel GA search algorithm we present offers much faster convergence than prior GA methods, while the new robust evaluation metric ensures more precise alignments, even in the presence of significant noise, than mean squared error or other well-known robust cost functions. The paper presents thorough experimental results to show the improvements realized by these two contributions.

Index Terms—Range image registration, genetic algorithms, robust methods, stochastic search.

1 Introduction

Range image registration has been applied in many research areas, including medical imaging, robotic vision, and archaeology [1]. Most applications focus on developing techniques to construct precise 3D object models, preserving as much information as possible [2]. Recently, projects such as the Digital Michelangelo [3] and the Great Buddha [1] in digital archaeology have presented new challenges. A primary objective of these efforts is the digital preservation of cultural heritage objects before degradation or damage caused by environmental factors, erosion, fire, flood, or human development. Also, some collaborative efforts have supported the repair and restoration of historic buildings, construction of virtual museums, teaching using 3D visualization, and the analysis of complex structures by their 3D models [3], [4].

Multiple scans from different viewpoints are required to construct 3D models of physical objects [5], [6], [7], [8], [9]. The 3D model is then built by aligning and integrating these range images. These two basic steps can be performed simultaneously or sequentially.

The simultaneous methods [8], [10], [11] are generally considered to be more robust at reaching precise 3D models. In this category, a global registration between all pairs of views is performed, followed by their integration. The accumulated error between the previously registered views is distributed among all alignments to limit model distortion while preserving the geometry. Although these methods have shown success in a number of cases, they have some drawbacks including their computational complexity and the loss of small details owing to imprecise alignments or error accumulation.

Usually, sequential methods [12], [13] produce imprecise object models since the transformations errors accumulate and propagate from one iteration to another. However, if one can guarantee precise alignments, this method is more attractive because it requires fewer computational resources (i.e., memory) than the other. Regardless of the approach (sequential or simultaneous), it is important to minimize the number of views needed to construct the model because data acquisition can be very expensive [1] and because we need to limit error accumulation in the resulting model.

The goal of the registration task is to find the transformation that best represents the relative displacement between two surfaces having a common overlapping area. The efficient estimation of this transformation is a central issue in registration [14], [15]. Range image registration methods may be distinguished by the techniques used to identify corresponding features and by the method of estimating the transformation between the views.

Registration approaches can be classified broadly into two distinct classes: *coarse* and *fine*. The goal in coarse registration is to find a set of approximate registration transformations without prior knowledge of the relative spatial positions of the views. Most of these methods are

- *L. Silva and O.R.P. Bellon are with the Departamento de Informática, Universidade Federal do Paraná, Caixa Postal 19092, Curitiba, PR, Brazil 81531-980. E-mail: {luciano, olga}@inf.ufpr.br.*
- *K.L. Boyer is with the Department of Electrical and Computer Engineering, The Ohio State University, Columbus, OH 43210-1272. E-mail: kim@ece.osu.edu.*

Manuscript received 8 May 2003; revised 21 Sept. 2004; accepted 13 Oct. 2004; published online 11 Mar. 2005.
Recommended for acceptance by A. Rangarajan.
For information on obtaining reprints of this article, please send e-mail to: tpami@computer.org, and reference IEEECS Log Number TPAMI-0068-0503.

based on finding correspondences between distinctive features that may be present in the overlapping area. The basic procedure involves the identification of features, assignment of feature correspondences, and computing an alignment based on these correspondences. There are many different features that can be explored: edge maps [16], lines and planes [17], bitangent curves [18], surface curvatures [19], [20], surface orientation [21], and invariant features, such as moments and curvature [5].

Coarse registration methods generally supply only rough alignments. In contrast, fine registration techniques are based on the assumption that a good initial transformation (i.e., reasonably close to the solution) is already known. Then, precise alignments may be obtained under suitable criteria. A number of registration approaches in the literature combine both techniques, with coarse registration followed by fine registration, to achieve automatic registration results [8], [16], [22].

The best-known methods for fine range image registration are variations on the Iterative Closest Point (ICP) algorithm [23]. A landmark contribution when first introduced, ICP is an iterative procedure minimizing the mean squared error (or the sum of squared distances) between points in one view and the closest points, respectively, in the other. At each iteration, the geometric transformation that best aligns the two images is calculated. The proper convergence of ICP is guaranteed only if one surface is a subset of the other; otherwise, erroneous alignments can result.[1] Another drawback of ICP is that it requires a good prealignment to converge to the best global solution. Many variations of the ICP have been proposed to address these limitations, with varying degrees of success [5], [13], [24]. For partially overlapping views, heuristics have been proposed to confine ICP's attention to the overlapped regions to improve the results [24], [25].

One alternative is to find the geometric transformation through a pose-space search, rather than the correspondence-based search of ICP-based methods. In this case, the objective is to find, in a huge search space of geometric transformations, a solution acceptably close to the global optimum, in a reasonable time. One way to perform this search is through efficient stochastic optimization techniques, such as genetic algorithms (GAs) [26] or simulated annealing (SA) [27]. This approach is generally regarded as providing coarse registration. However, one can combine different operators, such as local search heuristics, to obtain precise alignments. In that way, the final registration results can compare favorably with traditional fine registration approaches. Other pose-space search approaches have been proposed for registration applications in the medical field using calibrated acquiring systems [28], [29].

GAs are computational models of natural evolution in which stronger individuals are more likely to be the winners in a competitive environment. GAs are simple and effective techniques for optimization problems in a variety of areas [26]. They are also intrinsically parallel. However, the main advantage of the GA approach for range image registration is that prealignment between views is not necessary to guarantee a good result. Yet, the GA is a stochastic method and generally time-consuming.

GAs have been successfully applied to image registration problems in several areas, including remote sensing [30], medical imaging [31], and others. Nevertheless, there exist many difficulties in developing reliable and automatic registration methods based on GAs to obtain precise alignment; this paper addresses these.

Brunnstrom and Stoddart [32] proposed a simple method for free-form surface matching that combines GAs with ICP. An initial alignment is estimated by a traditional GA, followed by ICP refinement to obtain a final registration. Although generally effective, this method can become trapped in a local optimum. Recently, an alternative range image registration algorithm based on a GA was proposed [33], using a parallel evolutionary registration approach. This method effectively avoids premature convergence in most cases. Of course, while the parallel implementation reduces computational time, its solutions are no more precise than standard GA methods.

This paper presents an extensive study of enhanced GA approaches for precision range image registration. We focus on the problem of obtaining precise alignments through a robust registration method using views that only partially overlap. To support this, we define and use a new robust measure, the Surface Interpenetration Measure (SIM), to calculate the interpenetration of two registered range views. Our results show that the combination of enhanced GAs (for search) with the SIM (for evaluation) produces more accurate registration than either traditional ICP-based methods or traditional genetic algorithms.

Some authors have conducted comparative studies of ICP variations [24], [25], but it is difficult to draw solid conclusions from these because they use neither a common image database nor well-defined metrics. In [24], the authors were focused on obtaining the fastest algorithm, while, in [25], robustness was the main topic of interest. We will present comparative results against three well-known "benchmark" ICP algorithms. The common lesson in these comparative studies is that, while ICP continues to undergo development and extension, progress on this front has become asymptotic; further improvements are likely to be incremental, at best. The characteristics of ICP that limit its effectiveness in domains where robustness is required and prealignment is infeasible remain. Occasionally, the strategies to overcome the prealignment limitation may guide the convergence process to an erroneous result [25]. What is needed is a fundamentally different search approach, including a robust assessment of alignment quality. While it is infeasible to implement all variants of the ICP, we believe that the implementations we consider, taken together with the cited work, afford an accurate assessment of ICP-based algorithms.

2 Surface Interpenetration Measure

In this section, we define a new robust measure of surface alignment. We present experimental evidence comparing the behavior of the SIM to that of classical mean-squared

1. We will use the terms "erroneous" and "incorrect" to describe alignments that are, in effect, completely wrong. Multiple alignments, all of which are basically "correct," will be distinguished in terms of their precision. The focus of this paper is on achieving alignments that are highly precise, not just "correct."

error, while deferring a full discussion of our alignment algorithm to Section 3. We also provide some theoretical insight into the action of the SIM and experimental evidence for its stability in the presence of noise.

One of the main difficulties in evaluating registration results is acquiring the "ground truth" registration of two views. Some papers present quantitative evaluation metrics applying randomly chosen transformations to one view from a pair of aligned views (usually obtained from synthetic range data) and performing the registration [24]. After registration the mean squared distance is computed between the points of the transformed view before the transformations and after the registration since the true corresponding points are known.

In registering real range images, the true point correspondences are difficult to obtain even through calibrated ranging systems [7], [34]. Therefore, erroneous alignments can generate a small interpoint error, giving a misleading (optimistic) measure because of the incorrect estimation of corresponding points. This error is usually computed by the mean squared error (MSE) between corresponding points of two images after the registration process.

Visual comparisons can provide a qualitative evaluation of registration using real range images. Dalley and Flynn [35] suggest that a good registration should present a large "splotchy" surface, which is the visual result of two surfaces, each rendered in a different color, crossing over each other repeatedly. This effect can be described as the *interpenetration* of the two surfaces. However, it is impossible to measure the degree of interpenetration by visual inspection alone. At best, we gain a qualitative assessment. Moreover, being a qualitative assessment, "splotchiness" provides no useful control mechanism to guide the registration process.

The interpenetration effect results from the nature of real range data, which presents slightly rough surfaces with small local distortions caused by limitations in the precision of the sensor or by noise. Because of this, even flat surfaces (e.g., a polished plate made of wood or metal) present some "roughness." With this, we can assume that, independently of the surfaces' shapes, some interpenetration of two overlapped views will always occur. Below we define a new measure that quantifies this interpenetration effect to identify precise alignments and to provide a highly robust control for range registration.

2.1 Definition

For a given alignment of two images, A and B, we identify the set of interpenetrating points in A with respect to B. For each point $p \in A$, we define neighborhood N_p to be a small $n \times n$ window centered on p. We choose $n = 5$ based on the observation that the interpenetration is a local effect. With q denoting a point in the neighborhood N_p, c the corresponding point of p in image B (computed by a nearest neighbor calculation using a k-d tree structure for search optimization [36]), and $\vec{n}_c$ the local surface normal at c, we define the set of interpenetrating points as:

$$C_{(A,B)} = \{p \in A \mid [(q_i - c)\cdot\vec{n}_c][(q_j - c)\cdot\vec{n}_c] < 0\}, \qquad (1)$$

where $q_i, q_j \in N_p$ and $i \neq j$. This set comprises those points in A whose neighborhoods include at least one pair of points separated by the local tangent plane, as computed at their correspondents in B; Fig. 1 illustrates.

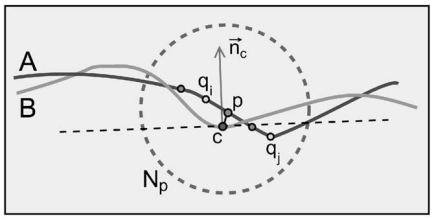

Fig. 1. Interpenetrating point p in A with respect to B.

With this, we then define the Surface Interpenetration Measure as the fraction of interpenetrating points in A:

$$SIM_{(A,B)} = \frac{|C_{(A,B)}|}{|A|}. \qquad (2)$$

A registration of two surfaces that presents a good interpenetration has a high SIM value. Our experimental results show that erroneous alignments produce low SIM values and that *small differences in MSE can yield significant differences in SIM*. Furthermore, alignments with high SIM present a very low interpoint error between the two surfaces. That is, the interpenetration measure is a far more sensitive indicator of alignment quality when comparing "reasonable" alignments.

Intuitively, it is possible to assess the quality of the registration result using both MSE and SIM without a visual verification. Of course, the SIM measure alone is not enough to determine if an alignment is correct, but it can confirm a good result when analyzed together with the resulting MSE.

2.2 Experimental Comparison: SIM versus MSE

We performed a number of experiments to compare the registration results using SIM *versus* MSE. The results indicate that the SIM is a robust, yet sensitive indicator of alignment quality for partially overlapped views. As we shall see, the SIM is most effective at refining *good* alignments to achieve *precise* alignments. For instance, a "correct" alignment with low MSE may exhibit no interpenetration if the aligned surfaces are parallel but slightly displaced. However, by maximizing the SIM, we can reach a precise alignment while preserving a low MSE. Other authors have reported that there may exist several local solutions for "good" alignments when the registrations are evaluated by MSE [5], [8].

Fig. 2 illustrates how MSE may fail to indicate the most precise registration.

To evaluate and compare the SIM *versus* MSE, we performed a number of registrations using different combinations of views with unequal overlapping areas. Fig. 3 shows an example of two correct alignments in which approximately 55 percent of Fig. 3a overlaps the view in Fig. 3b, while approximately 75 percent of Fig. 3b overlaps the view in Fig. 3a.

Fig. 3c was produced by the "scanalyze" system.[2] This is perhaps the most popular available framework for range image registration and is being used in the Digital

2. Available at http://graphics.stanford.edu/software/scanalyze.

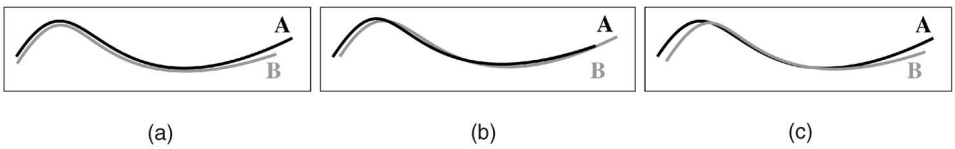

Fig. 2. Different alignments of two range images A and B, all with low MSE: (a) parallel surfaces, (b) surfaces that cross each other over different regions, and (c) misaligned surfaces presenting regions with very low MSE. The situation in (b) is the preferred (more precise) alignment, but it may not exhibit the lowest MSE among the three.

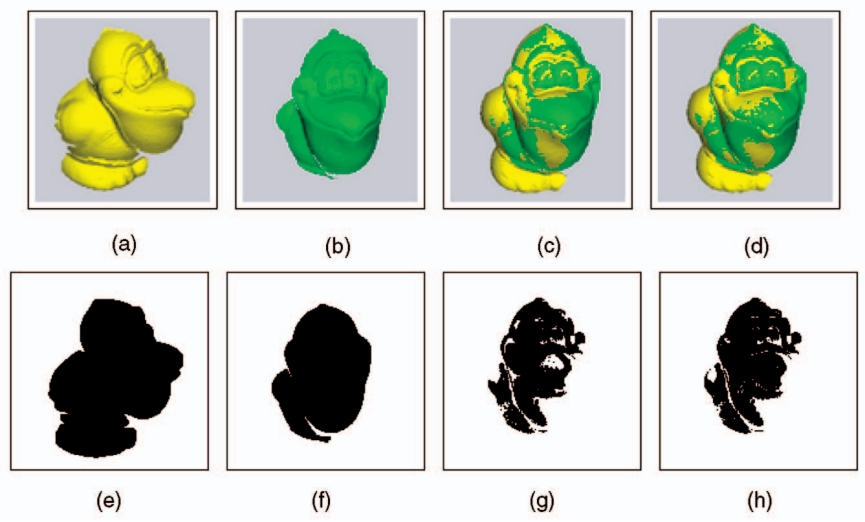

Fig. 3. Binary images from the SIM for the alignment between views (a) and (b). (e) and (f) are the respective binary images of (a) and (b), which represent valid points from the range data; (c) and (d) show the alignment obtained by ICP1 and by our robust GA-based method, respectively; (g) and (h) show the interpenetrating points from the SIM of the alignments in (c) and (d), respectively, with (f) serving as A in the SIM calculation.

Michelangelo project [3]. Therefore, it serves as a reasonable benchmark. In the scanalyze software, we tested a number of combinations of parameters and an average of best results were obtained by setting the normal-space sampling rate to 50 percent, the number of iterations to 20, rejection of the worst 3 percent of corresponding point pairs, rejection of corresponding points on the surface boundaries, and using the point-to-point error metric. All ICP registration results in this section were obtained in this way. We will refer to this implementation as "ICP1" throughout the paper to distinguish it from two other ICP implementations also tested in Section 4.

Fig. 3d was produced using the robust genetic algorithm implementation (explained below) with the surface interpenetration measure. Figs. 3c and 3d both show correct alignments having similar MSE values. Although the MSE of the ICP result is lower, the SIM shows that for the alignment of Fig. 3d approximately 4 percent more of the total valid points are interpenetrating than for Fig. 3c. This represents more than 250 of the 6,309 points of the surface of the object of Fig. 3b.

The MSE-driven results generally present a low global registration error, but the spatial distribution of this error is not uniform. For instance, the registration in Fig. 3c presents a very slightly lower MSE, but there are regions without interpenetrating points where the surfaces are parallel. MSE is calculated for corresponding points. Therefore, any alignment based on minimizing this quantity should reveal a very low MSE between the corresponding points in the overlap region, and this is what one typically sees. Unfortunately, the notion of corresponding points is problematic in most range image registration problems because the two images invariably sample the overlapping portions of the surface differently. When one also considers changes in the relative orientation of the surface with respect to the sensor, it is clear that not only are the sample points different, even the sampling intervals across the surfaces will vary and will do so differently in the two images. MSE, as calculated for corresponding points, cannot account for this effect. *This is a significant source of the SIM's improvement over MSE in achieving precise surface alignments; it does not rely on pointwise correspondence.* The result in Fig. 3d illustrates a case in which a low MSE is maintained, but a very slight increase is tolerated to achieve the substantial improvement in interpenetration, resulting in a more precise alignment. As Fig. 3g shows, the binary image of interpenetration reveals gaps where the surfaces are locally parallel; the SIM-driven result closes many of these, as seen in Fig. 3h.

By analyzing local patches taken from correct alignments, we can confirm that maximizing the SIM better distributes the registration error over the common regions. Recall that the two alignments of Fig. 3 show very similar global MSE values. Fig. 4 shows two local patches taken from these two alignments. Fig. 4a presents the interpenetration image from the MSE-optimized (ICP1) result; Fig. 4b presents that of the SIM-optimized (robust GA) result. In the area bounded by the red (left) box, the (local) MSEs of the two alignments are almost identical, and both results show good (local) interpenetration. In this area, the two alignments are very similar, and we believe that the two sets of surface samples are nearly congruent here. In the area bounded by the green

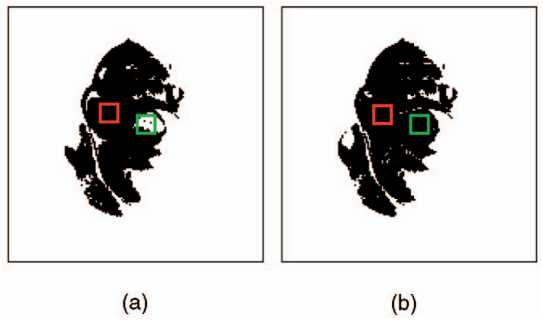

Fig. 4. Comparison of binary images from the SIM for the alignment of Figs. 3c and 3d on different regions: (a) Within the left box region, the MSE = 0.062905 and, within the right box region, the MSE = 0.137839; (b) within the left box region the MSE = 0.063036 and, within the right box region, the MSE = 0.093385.

(right) box, the MSE-driven result shows poor interpenetration, while the SIM-driven result shows good interpenetration. In this area, the (local) MSE of the (global) MSE-optimized result is considerably worse (more than 47.5 percent higher) than that of the SIM-optimized result. This reveals the benefit of allowing the global MSE to rise slightly while distributing the error more uniformly over the alignment. The MSE simply has no mechanism to account for the spatial distribution of the error.

We next computed the MSE and SIM numbers incorporating the constraints corresponding to the scanalyze (ICP1) method. That is, in (re)computing these values, we eliminated corresponding points on the surface boundaries (constraint cs_1, as defined in [24]) to limit erroneous correspondences. Under constraint cs_1, the SIM and MSE results for the alignments in Fig. 3 are: (c) MSE = 0.2539 and SIM = 64.08 percent, (d) MSE = 0.2546 and SIM = 68.07 percent. This again illustrates that the SIM is more discriminating than the MSE in that it "interlocks" the surfaces over more of their overlapping area. Constraint cs_1 proves to be very efficient at avoiding erroneous correspondences; it improves the SIM results, as well, and we will exploit this below.

To further explore the "interlocking effect" on the MSE of a SIM-driven result, we modified the experiment to calculate the interpoint error only over regions of interpenetration (over all such regions). The MSE values calculated only over the interpenetrating points are 0.6368 for the (global) MSE-optimized result in Fig. 3 and 0.5789 for the SIM-optimized result. If we include the 8-neighbors of interpenetrating points in the calculation, we get MSE values of 0.9203 (c) and 0.8649 (d). If we also introduce constraint cs_1 into this calculation, the respective results are 0.25889 (c) and 0.24921 (d) without 8-neighbors and 0.26141 (c) and 0.25775 (d) with 8-neighbors of interpenetrating points included. Altogether, these results confirm that optimizing the SIM produces superior MSE in those regions of interpenetration than does the global optimization of MSE.

Figs. 5 and 6 show two more examples of correct registration comparing the MSE and SIM values. For both examples, the SIM was calculated under constraint cs_1. The results for Fig. 5 overall are: (c) MSE = 0.4454 and (d) 0.4923; when using only the interpenetrating points, we get (c) MSE = 0.4356 and (d) 0.3871. The results for Fig. 6 overall are: (c) MSE = 0.1794 and (d) 0.1905; using only the interpenetrating points, we have (c) MSE = 0.11638 and (d) 0.11557. Again, we see that optimizing the SIM overall serves to improve the MSE slightly in those regions where interpenetration occurs.

2.3 Theoretical Support for the SIM

The preceding subsection offers experimental support for the SIM over the MSE and has provided us with clues as to the source(s) of its advantage. The advantages discussed to this point have to do with the spatial distribution of the alignment error and the inconsistent sampling of the surfaces. Those observations only tell part of the story. Now, we establish another, theoretical basis of support for the SIM over MSE in the alignment "end game." To do so, we test the following hypothesis:

> *The Probabilistic Error Distribution is Not Gaussian.* As the process enters the final stages of alignment, the errors are not well-approximated as conforming to a Gaussian distribution.

While optimal in the presence of Gaussian errors, it is well-known that the mean squared error leads to highly misleading results when the disturbances are not Gaussian.

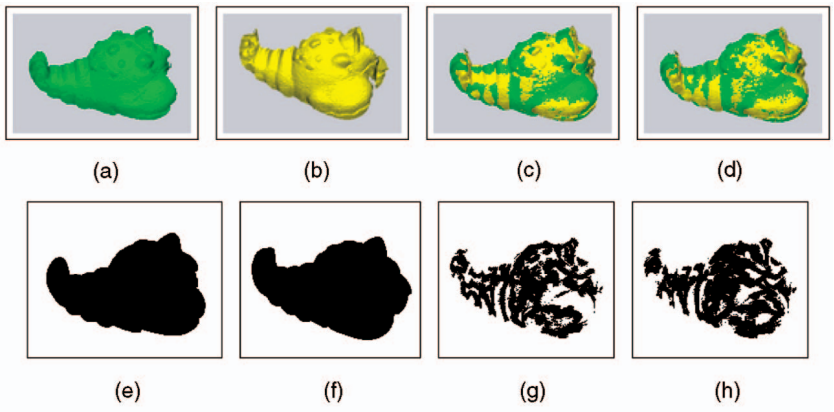

Fig. 5. Binary images from the SIM for the alignment between views (a) and (b). (e) and (f) are the respective binary images of (a) and (b), which represent points in the surface of the object; (c) and (d) show the alignment obtained by ICP1 and by the robust GA method, respectively; (g) and (h) show the SIM of the alignments in (c) and (d), respectively, with (f) as A in the SIM calculation.

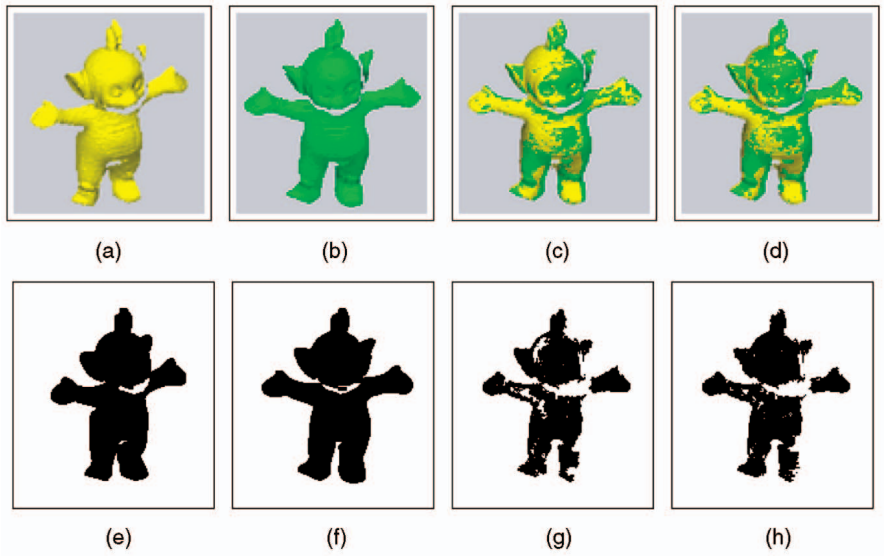

Fig. 6. Binary images from the SIM for the alignment between views (a) and (b). (e) and (f) are the respective binary images of (a) and (b), which represent points in the surface of the object; (c) and (d) show the alignment obtained by ICP1 and by the robust GA method, respectively; (g) and (h) show the SIM of the alignments in (c) and (d), respectively, with (f) as A in the SIM calculation.

This observation has driven a great deal of work in robust estimators.

As the registration process converges, the views are well-aligned and the error of corresponding points in the overlap area between views is very low. These errors can be computed by an interpolation using a point-to-plane correspondence search method [13] or by using a traditional point-to-point approach. We used the point-to-plane approach in this experiment to eliminate possible incorrect pairings, as suggested in [24]. However, our experiments show that, even with a point-to-point search approach, the configuration of corresponding points in the overlapping area is similar. The point-to-plane algorithm works by finding the corresponding point q in the image B that is closest to a line through the point p in the image A in the direction of its estimated surface normal at p. The idea is that this should generally be a better correspondent than the nearest point in Euclidean distance alone.

To test if the distribution of the errors in the overlap area is normally distributed, we used the chi-square (χ^2) test for normality [37], one of the most commonly used nonparametric statistical tests. The χ^2 test is used to compare a distribution observed in the data against another distribution determined by a hypothesis. Our hypothesis is that the probabilistic error distribution in the overlap area is not Gaussian. To use the χ^2 test, we pose the counter hypothesis, that the errors are Gaussian. If the Gaussian hypothesis is rejected, then we have proven our point.

The basic idea to prove or disprove this hypothesis using the χ^2 test is to divide the n error values in the overlapping area into k cells and compare the observed number in each cell with the expected number of a normal (Gaussian) distribution with:

$$\chi^2 = \sum_{i=1}^{k} (O_i - E_i)^2 / E_i, \tag{3}$$

where O_i is the observed frequency for cell i and E_i is the expected frequency for cell i. One can automatically compute the ratio n/k, which should be at least 5. In our experiments, $k = \lfloor 4[0.75(n-1)^2]^{1/5} \rceil$, as in [37].

The (counter) hypothesis of normality is rejected at an α level of confidence (usually 95 percent) if the computed value of χ^2 is greater than a pretabulated critical value of χ^2 with $k-1$ degrees of freedom.

We applied the χ^2 test to more than 300 well-aligned view pairs obtained from ICP approaches and from our methods. For all registrations, no matter the technique, the hypothesis of normality was rejected, even at low confidence levels. Moreover, the histograms of the error distributions reveal that the errors are not normally distributed; they exhibit thick tails. This indicates the need for a robust measure and the SIM fills this role.

2.4 Noise Rejection

To show that the SIM is stable in the presence of noise, we performed experiments using noisy surfaces. Given two registered views, we add to both views the same amount of noise and compute the SIM. This experiment was performed on several registration results and for different noise types and levels, that is, Gaussian noise, salt-and-pepper (S&P) noise, and a combination. In this experiment, the noise was added *after* registration to show the stability of SIM with respect to noise for a given surface alignment. Registration results for noisy surfaces to illustrate the robustness of the search algorithm using the SIM, appear in Section 3.

For all cases in this paper where S&P noise is introduced, we set the amplitude range of the noise equal to the z dynamic range of the image. For example, if the z values in the "clean" image range from -20 to +50, the value of a given perturbation is drawn at random from $[-35, 35]$. The level of the S&P noise, expressed as a percentage, is the fraction of original pixels to be perturbed, chosen at random.

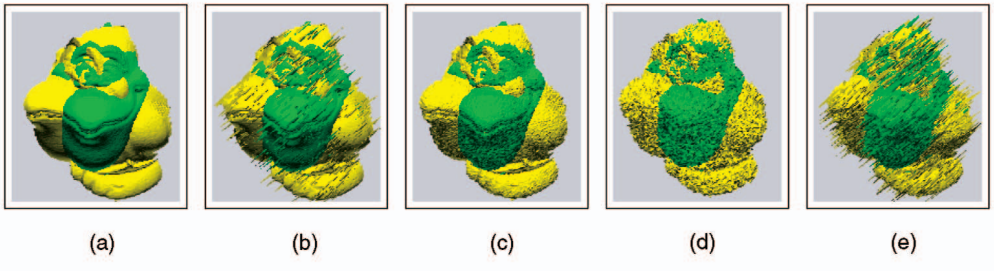

Fig. 7. Views with different noise types and levels: (a) initial alignment without noise; (b) 5 percent S&P noise; (c) Gaussian noise, $\sigma^2 = 0.01$; (d) Gaussian noise, $\sigma^2 = 0.1$; (e) Gaussian noise, $\sigma^2 = 0.01$, plus 10 percent S&P noise.

Gaussian noise has very little influence on the SIM of erroneous alignments. For correct alignments, the SIM actually increases with high noise levels because the surface roughness increases with the noise, thereby increasing the number of interpenetrating points. S&P noise exerts more influence on the SIM because many of the noisy pixels of one surface pierce the other, thus increasing the interpenetration, even for erroneous alignments. This effect can produce a significant increase in the SIM. To minimize the impact of S&P noise, we introduce a constraint C_m into the SIM calculation. C_m can be represented as the maximum distance allowed between a pixel $q \in N_p$ and the tangent plane at c, as presented in (1) in Section 2.1. In our experiments, $C_m = 0.5$, representing approximately 1 percent of the range of values in these data sets, was enough to suppress the effect of this noise. Fig. 7 shows an example of the erroneous alignment with different noise realizations to illustrate its influence on these images.

Fig. 8 illustrates the behavior of the SIM with respect to noise level for a correct and an erroneous alignment. In this plot we present three different tests: 1) Gaussian noise only, 2) Gaussian noise plus 10 percent S&P noise, and 3) as in test 2 but including the constraint $C_m = 0.5$ in the SIM calculation. This experiment shows that the measure remains stable over a wide range of noise levels (notice the logarithmic scale on the horizontal axis). This is particularly, and importantly, true for erroneous alignments. It is therefore highly unlikely that noise effects will cause a poor alignment to masquerade as a good one under the SIM. Moreover, the use of constraint C_m overcomes most of the noise influence. This experiment underscores the SIM's ability to provide a robust indication of alignment quality highly immune to noise, sensor error, and other perturbations.

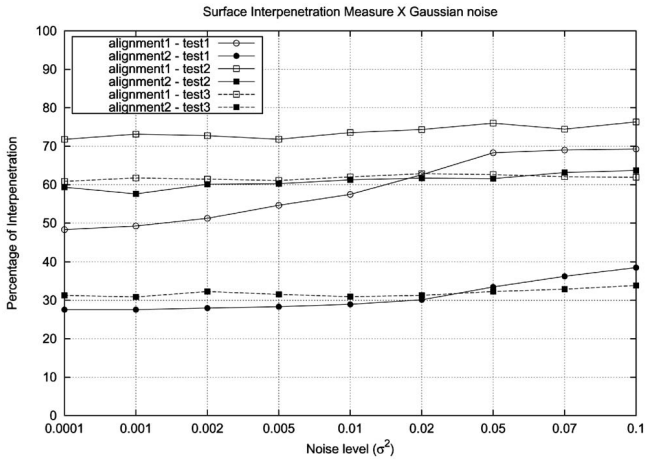

Fig. 8. Surface Interpenetration Measure against different noise levels. Alignment1 is a correct registration; Alignment2 is an erroneous registration. The measure is stable for noise levels covering three orders of magnitude, particularly—and importantly—for erroneous alignments.

3 Genetic Algorithms for Range Image Registration

From their introduction by Holland [38] and popularization by Goldberg [39], the behavior of genetic algorithms has been explained by making reference to the biological metaphor of evolutionary adaptation.

The general principle underlying GAs is to maintain a population of possible solutions (individuals) encoded in the form of a chromosome (a string of genes) and to submit the population to an evolutionary procedure until some criteria can be satisfied.

In the evolutionary procedure, each individual is assigned a fitness value provided by a user-defined fitness function; the fittest individuals have a greater chance of being selected for reproduction. With the intent of creating better individuals, the crossover operation exchanges the genes of each pair of chromosomes selected for reproduction. The created (offspring) chromosomes, before being introduced into the population, may undergo mutation, a random perturbation, to enrich the genetic material in the population. Mutation occurs with a very small probability such that the evolutionary process does not degenerate to a random search. At the end of the evolutionary process, the fittest chromosome is taken as the final solution.

To perform range image registration using a GA, we represent the possible solutions as a chromosome string defined by six genes—the three parameters each of rotation and translation relative to a 3D coordinate system. The chromosome's genes store the parameters of a geometric transformation that, when applied to one view, can align it with the other. The objective of the evolutionary process is to find the best geometric transformation (chromosome) possible in a population of individuals.

The population of the GA is usually initialized randomly, with each gene set within a range of values based on the image size. To reduce the domain for translations, we translate the views to the origin of the coordinate system using their centers of mass. In Section 4, we explain in detail the setting of GA parameters.

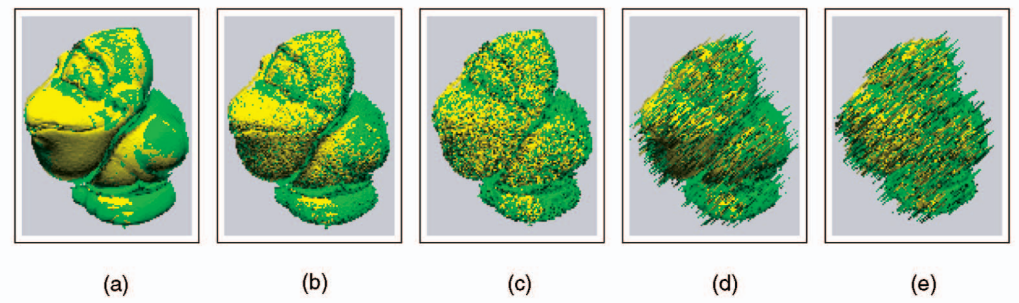

Fig. 9. Registration results obtained by our GA using cost function f alone (no SIM), for different noise types and levels: (a) without noise; (b) Gaussian noise, $\sigma^2 = 0.01$; (c) Gaussian noise, $\sigma^2 = 0.1$; (d) 10 percent S&P noise; (e) Gaussian noise, $\sigma^2 = 0.1$, and 10 percent S&P noise.

3.1 The Fitness Function

Initially, we define a fitness function based on the sum of squared distances between (the most nearly) corresponding points of two registered images.[3] This function uses outlier rejection based on the MSAC robust estimator [40] and, recently, we applied a similar fitness function to the range image segmentation problem with success [41], [42]. A chromosome's fitness value is given by a cost function f:

$$f = \frac{1}{N}\sum_{i=1}^{N}\rho(r_i), \tag{4}$$

where N is the number of points in image A, with $A = \{a_i\}$. The robust residual term ρ is denoted by:

$$\rho(r_i) = \begin{cases} r_i & \text{if } r_i < t \\ t & \text{otherwise.} \end{cases} \tag{5}$$

where t is a defined threshold and r_i is defined as:

$$r_i = \|b_i - Ra_i - T\|^2, \tag{6}$$

where b_i is the closest point in image B to the point a_i, with $B = \{b_i\}$. R is the rotation matrix and T the translation vector, given by the chromosome's genes. The threshold t defines the maximum distance between a corresponding pair of points to be considered inliers. The inliers are generally those points in the overlapping area of the aligned views.

Using this approach, we can find the alignment that minimizes the sum of squared distances between corresponding points while maximizing the number of inliers. The objective is to find the alignment having the minimum value of f. In our current experiments, we set the threshold $t = 5$ (representing approximately 10 percent of the range of values).

Using the cost function f (alone) in a traditional GA, we obtained reasonable registration results, even with low-overlap views. We also performed experiments with noisy surfaces to confirm the robustness of f and the efficiency of the genetic search algorithm. In these experiments, different noise types and levels were added to both views *before* registration. Fig. 9 shows an example of registration results obtained by the GA using views at 0 and 20 degrees of the same object for different noise levels. The fitness values are: Fig. 9a $f = 0.409$; Fig. 9b $f = 0.422$; Fig. 9c $f = 0.518$; Fig. 9d $f = 0.733$; Fig. 9e $f = 0.854$.

3. The SIM will be introduced to the algorithm in due course.

3.2 Enhanced Genetic Algorithms

The previous results are reasonable, especially given the noise. However, the focus of this work is on precision. To reduce the interpoint error and, consequently, improve the quality of the alignment between views, it is necessary to enhance the GA. In fact, GAs are efficient at finding promising areas of the search space, but are not so efficient at fine scale search within those areas. In practical terms, GAs can reach a solution close to the global optimum in a reasonable time, but a great deal of time may be required to improve the solution significantly beyond this point.

In this context, local search heuristics such as hillclimbing can be combined with a GA algorithm to mitigate this problem [43]. Hillclimbing attempts to improve the result by moving directly toward a better, neighboring solution, within a predefined number of tries. Our GH method, a hybridization of GAs and hillclimbing heuristics, produces better results than traditional GAs. In GH, hillclimbing is applied after each generation to the individual with the best fitness value.

In the hillclimbing procedure, a gene from the best chromosome is randomly selected and an offset value selected at random from $[-c, c]$ is added to it. This hillclimbing procedure is analogous to "shaking" the two surfaces, seeking a better alignment in a predefined neighborhood of the best chromosome. If a better chromosome is found through the hillclimbing procedure, then it is added to the new population.

To isolate the impact of hillclimbing on convergence rate, Fig. 10 presents a comparison, averaged over multiple tests, for GH versus the standard GA (no SIM). The maximum number of attempts in the hillclimbing procedure was fixed at 10. This plot shows that $c = 0.5$ (representing approximately 1 percent of the range of values) offers the best results. Using $c = 2.0$ provided a rapid initial convergence, but insignificant improvement in later iterations. We postulate that this results from too much "shaking" of the surface as we near the solution.

This experiment suggests that dynamic settings for the offset range, taking large values in early generations and then gradually decreasing, may be even more effective. This is similar to the "cooling schedule" in simulated annealing (SA) [27]. We used this idea to enhance the GH method, computing the hillclimbing offset range dynamically. The offset range at generation g, $[-c_g, c_g]$ is given by:

$$c_g = T_{max} - g\left(\frac{T_{max} - T_{min}}{G_{max}}\right) \tag{7}$$

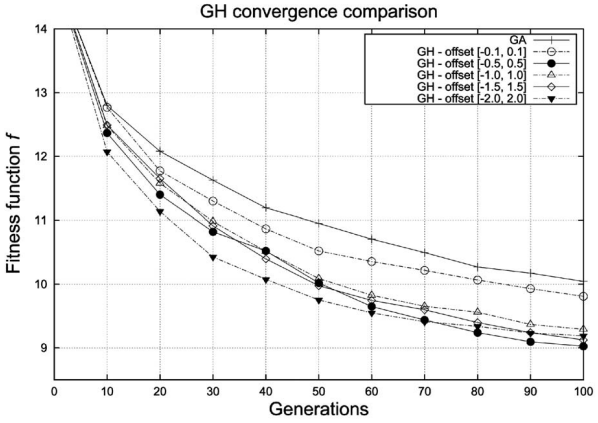

Fig. 10. Average of fitness function f obtained in the range image registration of different views within 100 generations using a different range of offset values in the hillclimbing procedure. "GA" refers to a standard GA with no hillclimbing and no SIM.

with G_{max} the maximum number of generations, g the current generation, and T_{min} and T_{max} predefined thresholds, with $T_{min} \leq c \leq T_{max}$. With this new approach, we obtain precise solutions in reasonable time, although the results are not materially different than with fixed-range hillclimbing. Therefore, all "GH" results from this point in the paper are generated with a fixed range of $[-0.5, 0.5]$.

We conducted experiments to compare these three approaches (Standard GA, GH, SA) to the range image registration problem. The SA implementation was based on Ingber's work [44] and the parameters of the SA used are the defaults of Ingber's VFSR library. We only eliminated the maximum number of times that the cost function repeats itself to try to prevent exiting prematurely at a local optimum. In this experiment, we computed the average of 10 runs for each approach using the same cost function defined in (4).

We compare on the basis of the time required and quality of the solution. The results show that SA converges very quickly to reasonable solutions, but may be unable to improve significantly on that result with time. In contrast, the standard GA converges more slowly but is able to improve the solution consistently (if not dramatically) with time. GH consistently outperforms the other two options. Table 1 presents the cost values of the results from each run to illustrate the improvements realized by the GA, which returned slightly better solutions than SA.

TABLE 1
Cost Value of Solutions for SA, Standard GA, and GH for 10 Runs

Run	SA	Std. GA	GH
1	0.926811	0.926424	0.918995
2	0.926813	0.925723	0.918651
3	0.926835	0.922001	0.918807
4	0.926810	0.920769	0.918647
5	0.926912	0.923867	0.918691
6	0.926818	0.922591	0.918646
7	0.922841	0.928005	0.918613
8	0.931059	0.924517	0.918841
9	0.926816	0.946007	0.918833
10	0.927034	0.923040	0.918920
Average	0.926874	0.926294	0.918764

3.3 Hybrid GA with Robust Cost Function

Our results to this point indicate that the GH converges efficiently to a good solution, as measured in terms of f. In Fig. 11, we plot f versus the SIM for average results produced by the genetic search algorithms as they run. (Recall that f is based on the MSE, with outlier rejection.) Evolutionary progress is from right (bottom) to left (top) on the plot. That is, solutions taken from early in the process exhibit large values of f (which we seek to minimize) and small values of SIM (which we seek to maximize); solutions taken late in the process show small f values and large SIM values. Notice that, as the gene pool evolves, the early solutions improve rapidly with respect to f, while the SIM remains relatively unchanged. In this region of the curve, f provides a sensitive, effective measure of progress. Later in the process, the SIM shows dramatic change as f stabilizes. Here, in the "end game," the SIM provides the more sensitive, effective measure of solution quality. By combining these two measures, we can obtain a more reliable, robust, precision registration process.

Based on this observation, we developed another cost function, g, using the surface interpenetration measure to compute the fitness value of each solution. Because we cast GAs as a minimization problem, $g = 1 - SIM_{(A,B)}$. Clearly, the surface interpenetration measure cannot be used until the alignments are reasonable because it is not an effective measure of progress in the early stages (see Fig. 11). In fact, until the surfaces begin to intersect, the SIM tells us nothing at all. So, we use f to evaluate the fitness of individual chromosomes early in the process. Later, as the surfaces become aligned, we switch to the SIM-based fitness function, g, which is more sensitive and leads to more precise, robust registration in the end. We define a

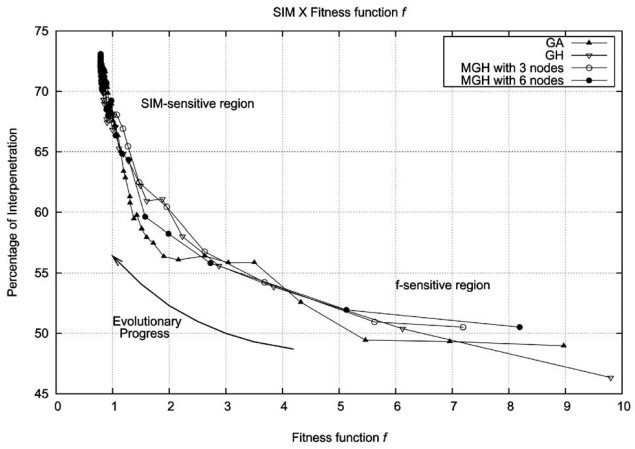

Fig. 11. Fitness function f versus SIM measures obtained by the average results of different GA approaches to range image registration. "MGH" refers to a parallel-migration GH implementation, provided for comparison. Migration approaches use multiple processors for increased speed [26].

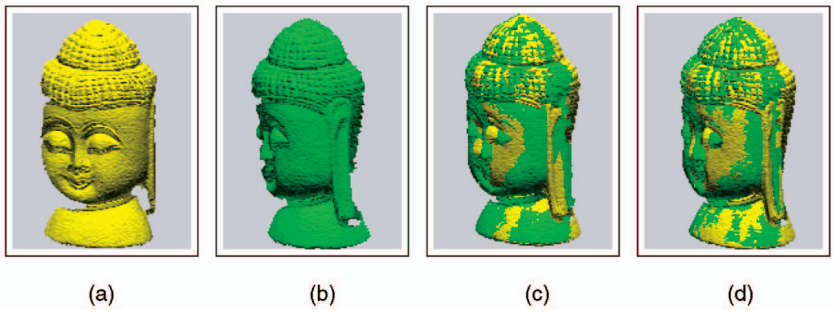

Fig. 12. Registration results from different views, (a) and (b) of the same object (views 0 and 40 degrees): (c) ICP1 convergence to an erroneous result; (d) correct registration with the GH technique (genetic algorithm with hillclimbing).

threshold n on the number of iterations to decide when to switch cost functions. It should also be possible to make a switching decision based on convergence rate, but we haven't done that.

Our experimental results show that $n = 90\%$ initial generations was enough to achieve good convergence results using the fitness function f. It is important to maintain a high value for n to guarantee good solutions. Also, we noticed that, in just a few generations from a reasonable starting point, the fitness function g can reach a very good solution. This approach was successfully applied on each of our genetic search methods.

The evaluation process of these GA-based methods, finding the corresponding point pairs between views and computing the mean of their Euclidean distances, is very time-consuming. The average time to align view pairs, each one having approximately 10,000 3D points, takes about five minutes on a 1.7GHz Pentium IV processor. We performed some experiments in which we reduced the number of 3D points by using sampling techniques [24] early in the process to accelerate the search. The idea is to evaluate a small portion of points at the beginning of the evolutionary procedure and to increase the number of sampled points near the end of the GA process. By reducing the number of correspondence searches at the beginning, when the views are not precisely aligned, one can significantly improve the speed of the GA-based methods while maintaining good results. Of course, the computational time of GAs can be significantly reduced if the process runs in parallel on a cluster of machines [33].

4 Experimental Results

The experimental tests were performed using the OSU SAMPL range image database[4] acquired with the Minolta Vivid 700 scanner. Each object in the database has been imaged in 18 views acquired at 20 degree intervals using a computer-controlled turntable. Each view contains approximately 9,000 points. For some view pairs, regardless of the specific variation implemented, ICP failed to achieve a reasonable alignment unless the views overlapped significantly and a good initial prealignment was supplied (see Fig. 12). The GA-based approaches suffered no such problems. Given this observation, we confined our comparative study of alignment precision to the first three contiguous views of each of five objects, totaling 15 test image pairs, three per object, as shown in Fig. 13. We performed all registrations without prealignment using the starting position of the views, as in Fig. 13. This somewhat restricted angular range allowed the ICP implementations to converge to a correct solution for this set of test images.

For comparison, we implemented a number of variants of the ICP algorithm [24] using both a software test-bed described in [35], [25] and, as noted above, perhaps the most popular framework for range image registration used in the the Digital Michelangelo project [3], called scanalyze (recall, ICP1). Below, we present detailed comparative results for the top three ICP performers.

In [25], the authors presented a extension of their previous work [35] that included comparative analysis of traditional approaches such as Chen and Medioni's point-to-plane method [13] (we will call this ICP2 below), and a point-to-point approach [36] where the authors presented robust statistics and adaptive thresholding (computed automatically) to deal with outliers (we will call this ICP3 below). We also tested a robust method proposed by Masuda and Yokoya [45] that handles outliers well using a dynamically computed threshold. This method presented good results, but, because they were very similar to ICP3, we omit the details.

In general, when considering ICP variants, we find that it is effectively impossible to declare one specific approach the best because what is best depends on the class of images and the application. But, regardless of image type and application, we observed that the outlier rejection rules [24] (i.e., avoid boundary) are particularly effective; this supports the findings of others [25].

In comparing the point-to-point and point-to-plane methods [24], [25], we found that the point-to-plane method is quite efficient at driving ICP to convergence, but that the point-to-point measure is more effective when aligning views from more disparate alignments. The point-to-plane approach is susceptible to oscillation and, in such cases, can fail to converge to an acceptable solution. On the other hand, the point-to-plane measure appears to be less likely to be trapped in local optima. These conclusions are consistent with the findings in [25]. In those cases for which both approaches converge to a good solution, a comparison of the postregistration corresponding points configuration reveals that the results are very similar and the resulting MSE values are not significantly different. Moreover, the point-to-point results present better interpenetration overall. Finally, the point-to-plane measure is more expensive to compute.

4. Available at http://sampl.eng.ohio-state.edu. The database owners respectfully request acknowledgment for its use.

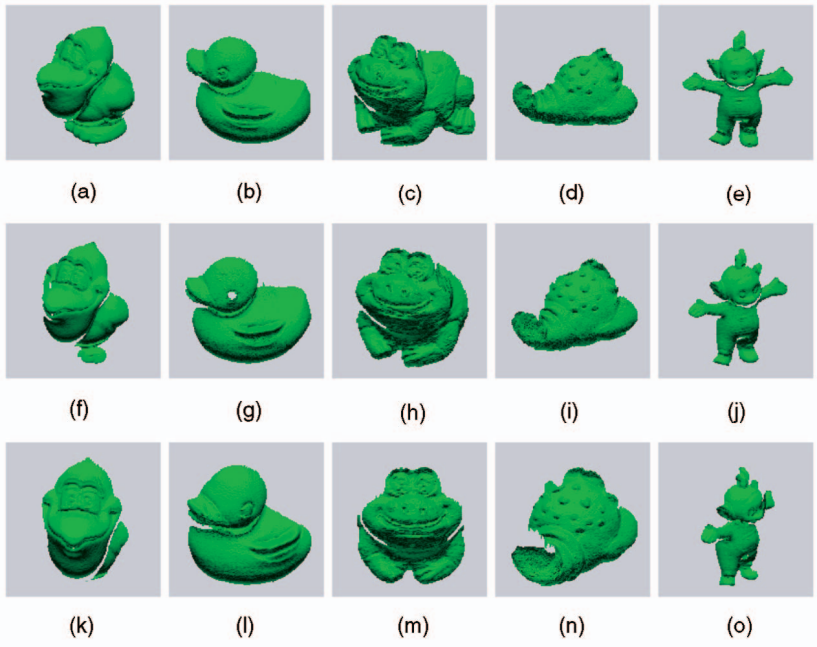

Fig. 13. The first three consecutive views of the five objects used in the experiments. The top line are views 0 degrees, in the middle are views 20 degrees, and the bottom are views 40 degrees.

Based on these observations, we have elected to use point-to-point error, which is less expensive to compute, for our GA-based registration methods as well. Experiments using point-to-plane as the corresponding point search method in our GAs show similar registration results and slightly lower interpenetration values.

In the comparative results below, we recompute the MSE of the entire alignment once the process (whichever one) converges. In this way, we ensure a fair comparison across all techniques.

For the genetic algorithms, we tested various parameter settings, such as population size, mutation and crossover probabilities, number of generations, selection rules, mutation rules, and others [26]. Based on the convergence times and quality of the solutions, we then fixed these parameters and ran a significant number of tests. Because genetic algorithms are stochastic methods, conclusions based on a few trials could be misleading. The robust GA uses both cost functions f and g within the GH search algorithm, while the "standard" GH uses only f (itself a robust estimator, of course). Therefore, the differences between GH and robust GA results reflect the impact of using interpenetration to guide the end of the registration process. We ran the registration method 50 times for each test image pair and calculated the average results.

The population size was set to 100 individuals, based on experience. Small populations (fewer than 50 individuals) tend to result in premature (erroneous) convergence, while very large populations (more than 200 individuals) converge very slowly. The termination condition was set to 100 iterations (generations). This combination of 100 individuals and 100 generations consistently yields reasonable solutions. The range of the three rotation parameters (X, Y, Z) were set within [-90, 90] degrees and the translation values were set within the greatest image sizes (width, height, and depth).

For mutation, we chose random selection over mutation by range, for improved genetic diversity. The probability of mutation equals 0.02 and the probability of crossover equals 0.9. We selected uniform crossover over point crossover, and the selection procedure was the tournament rule. At each iteration, we discard the 90 percent worst individuals (steady-state genetics) instead of replacing the entire population (generational replacement) as is done in standard GAs. Generational replacement produced very slow convergence. This "elitist" concept yielded improved convergence times without loss of population diversity.

Table 2 provides the recomputed final MSE, as well as the SIM, of each result. The novel robust approach (Robust GA) increased the SIM by approximately 7 percent over the original GH and by 11 percent over ICP for correct alignments. Recall that, while ICP is driven by MSE, GH and the early stages of the robust GA are driven by the cost function of (4), and the latter stages of the robust GA are driven by the SIM. Although the MSE of the ICP solution is usually lowest, the views were not always precisely aligned because the convergence is to a local optimum. Of course, these outcomes depend on the object complexity and the specific views in question. The SIM values of the ICP alignments support the claim that MSE is not the best measure to guide the *final* registration process. Figs. 14 and 15 offer a visual comparison of the registration results, showing that the robust algorithm using the SIM-based cost function g late in the convergence process represents a sensitive measure of precision in range image registration.

Figs. 16 and 17 illustrate, in one final test, the improvement offered by the robust genetic algorithm. The registration results appear in Fig. 16; the binary interpenetration images in Fig. 17. Fig. 16b shows the registration obtained by ICP1. While this is a reasonable alignment, Fig. 17b shows that there exists a large area with no interpenetration. The result of the "basic" GH (Fig. 16c and Fig. 17c)

TABLE 2
Comparative MSE and SIM Results

Test image	ICP1		ICP2		ICP3		GH		Robust GA	
pairs	MSE	SIM%	MSE	SIM%	MSE	SIM%	MSE	SIM%	MSE	SIM%
bird 0-20	0.4010	75.4	0.3993	69.8	0.3950	64.6	0.4175	86.5	0.4299	90.7
bird 20-40	1.3489	71.2	1.3395	67.7	1.2698	53.8	1.3709	77.3	1.4440	91.3
duck 0-20	0.6363	43.5	0.8309	35.4	0.7002	39.9	0.6558	46.8	0.8017	57.0
duck 20-40	0.8621	43.1	0.9060	38.2	0.8968	38.7	0.9055	46.1	0.9841	56.3
frog 0-20	0.3387	74.6	0.3402	75.4	0.3468	74.5	0.3410	75.7	0.3615	82.7
frog 20-40	0.7216	76.9	0.7933	76.1	0.8300	69.5	0.8186	79.2	0.8180	80.8
lobs. 0-20	1.0687	48.8	1.0553	47.2	0.9949	38.1	1.0721	51.0	1.2573	60.9
lobs. 20-40	3.3068	53.2	4.4498	55.0	3.1948	28.8	4.0016	50.4	3.9504	55.9
tele. 0-20	0.2275	82.3	0.2272	82.0	0.2270	80.9	0.2306	84.8	0.2393	91.0
tele. 20-40	0.4366	82.6	0.4378	83.8	0.4334	80.2	0.4392	86.5	0.4495	90.3
Average	0.9348	65.16	1.0779	63.06	0.9288	56.90	1.0252	68.43	1.0735	75.69

The first column shows the name of the objects in the database followed by the view numbers of each test pair. ICP1 represents a variant of ICP using the point-to-point approach (scanalyze). ICP2 has the same parameters as in ICP1 but uses the point-to-plane measure. ICP3 is Zhang's algorithm. GH is the genetic algorithm using f with hillclimbing; the Robust GA is our final algorithm using f (early) and g (late) in the search process.

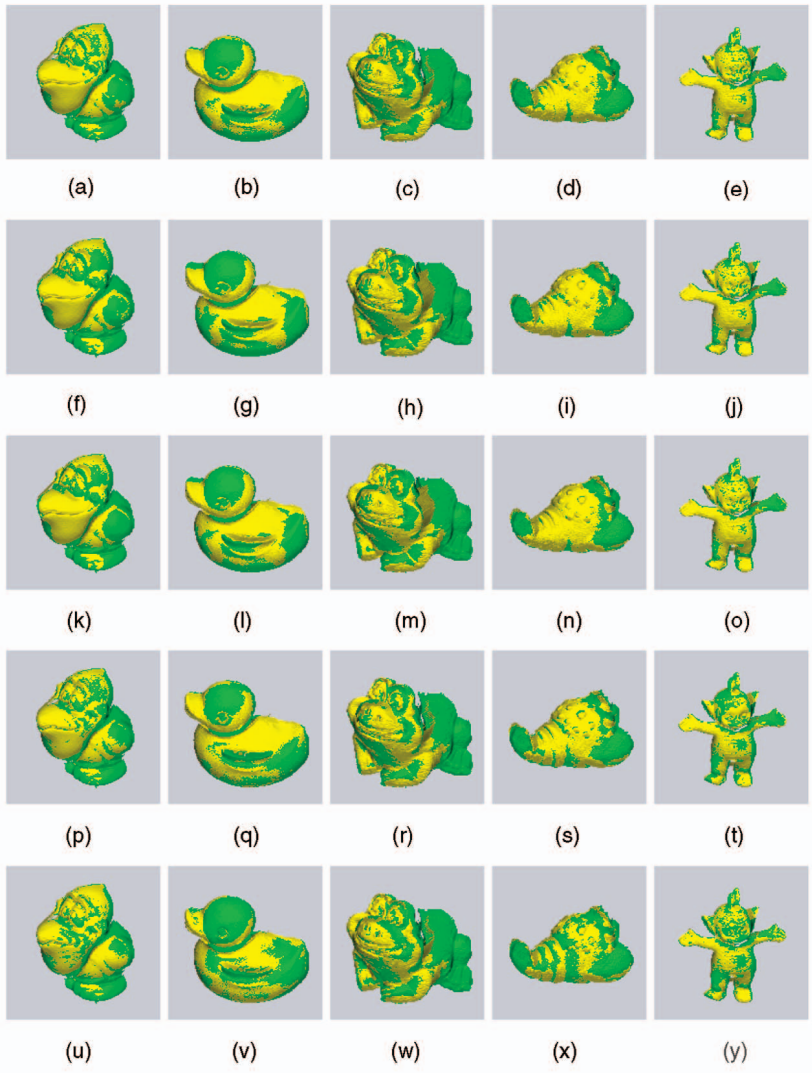

Fig. 14. Registration results of the test image pair 0-20 of the five objects used in the experiments. First row, ICP1; second row, ICP2; third row, ICP3; fourth row, GH; bottom row, robust GA.

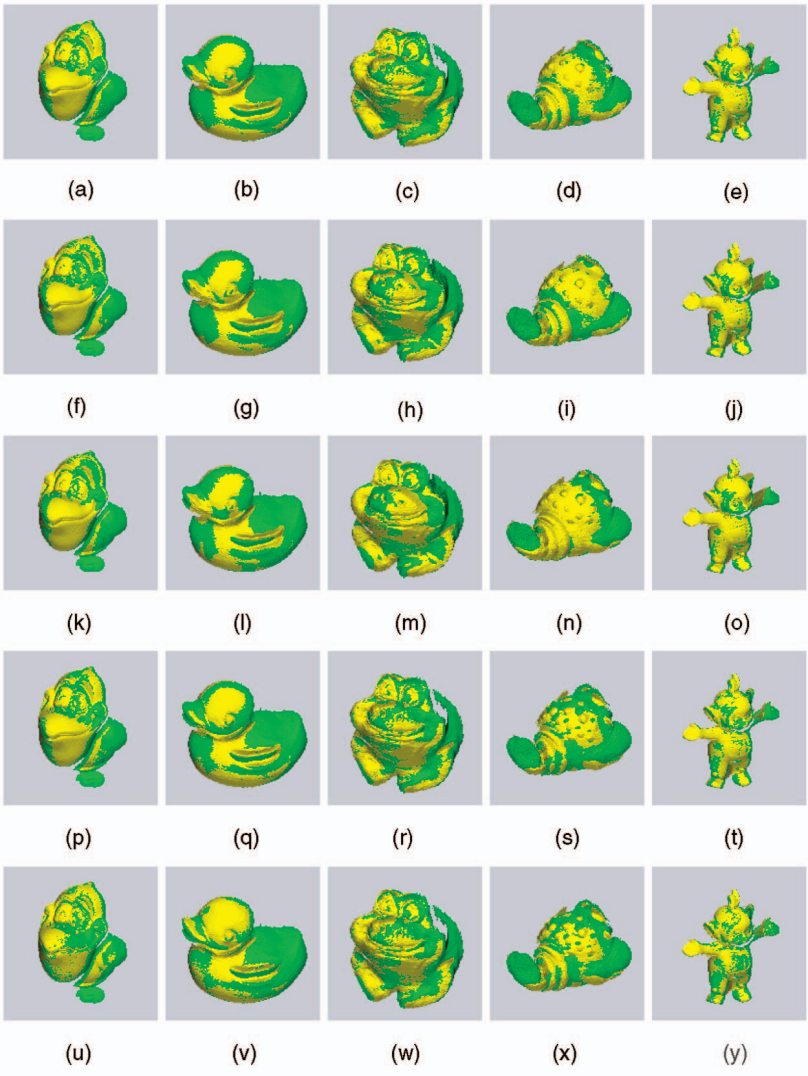

Fig. 15. Registration results of the test image pair 20-40 of the five objects used in the experiments. First row, ICP1; second row, ICP2; third row, ICP3; fourth row, GH; bottom row, robust GA.

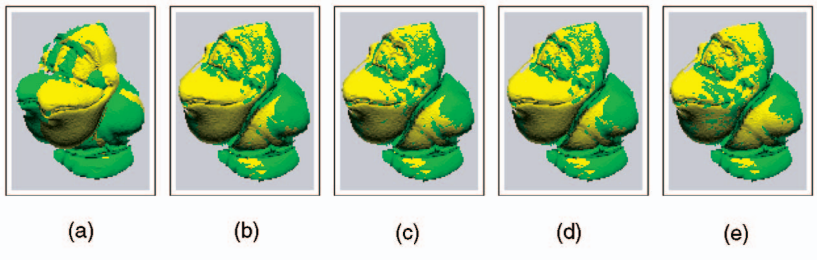

Fig. 16. Registration results: (a) initial views (0 and 20 degrees of a same object) MSE = 13.105, SIM = 29.45 percent; (b) ICP1 (MSE = 0.403, SIM = 75.427 percent); (c) GH (MSE = 0.414, SIM = 86.551 percent); (d) GH followed by ICP1 (MSE = 0.393, SIM = 65.88 percent); (e) Robust GA (MSE = 0.424, SIM = 90.79 percent).

shows superior alignment with more interpenetrating points. Testing the suggestion in [33], we applied ICP1 following the GH results in an attempt to improve the alignment. However, ICP1 still met a local minimum and the results are not acceptable. In fact, for this test, ICP1 actually *worsened* the alignment produced by GH (genetic algorithm with hillclimbing). The robust GA shows the best convergence results and greatest SIM values. The binary images of interpenetrating points (Figs. 17a, 17b, 17c, 17d, and 17e) show better homogeneity in distribution when a high interpenetration value is found, underscoring the effectiveness of the measure.

5 Final Remarks

This paper has presented an in-depth study of the range image registration problem and explores several genetic algorithm-based approaches to solve it. We developed a novel robust method for range image registration based on

Fig. 17. Binary images of the interpenetrating points (represented by white points) of each registration results in Figs. 16a, 16b, 16c, 16d, and 16e, respectively.

two key contributions: novel, hybrid genetic algorithms incorporating hillclimbing heuristics and a new performance measure, the Surface Interpenetration Measure (SIM), which we use in a new, robust fitness function. The results demonstrate the robustness of the SIM against different noise types and levels.

We confirm that this new measure is most useful in the final stages of "fine-tuning" the registration result. As the experimental results show, our method provides good performance in finding correct registrations with large interpenetrating areas. This is important in the construction of 3D models from multiple views, minimizing the error accumulation in the final model.

In choosing between ICP and our approach, the system designer has a number of issues to consider. Although our technique is clearly more robust, works for low-overlap conditions, and needs no prealignment, it must also be acknowledged that stochastic search techniques can be slow. In those domains for which speed is a premium or computational resources are limited and for which absolute precision is less significant, ICP may well be the preferred solution. For model-building, archaeology, and related domains, speed is (usually) less important than precision and robustness; our approach would be the method of choice in such cases.

Acknowledgments

The authors wish to thank the referees for their careful reading of the manuscript, and their many thoughtful comments. L. Silva and O.R.P. Bellon thank CAPES and CNPq for financial support.

References

[1] *Modeling From Reality,* K. Ikeuchi and Y. Sato, eds. Kluwer Academic, 2001.
[2] L.G. Brown, "A Survey of Image Registration Techniques," *ACM Computing Surveys,* vol. 24, no. 4, pp. 325-376, 1992.
[3] M. Levoy, K. Pulli, B. Curless, S. Rusinkiewicz, D. Koller, L. Pereira, M. Ginzton, S. Anderson, J. Davis, J. Ginsberg, J. Shade, and D. Fulk, "The Digital Michelangelo Project: 3D Scanning of Large Statues," *Proc. 27th Ann. Conf. Computer Graphics and Interactive Techniques,* pp. 131-144, 2000.
[4] F. Bernardini, I. Martin, J. Mittleman, H. Rushmeier, and G. Taubin, "Building a Digital Model of Michelangelo's Florentine Pieta," *IEEE Computer Graphics and Applications,* vol. 22, no. 1, pp. 59-67, Jan./Feb. 2002.
[5] G.C. Sharp, S.W. Lee, and D.K. Wehe, "ICP Registration Using Invariant Features," *IEEE Trans. Pattern Analysis and Machine Intelligence,* vol. 24, no. 1, pp. 90-102, Jan. 2002.
[6] C. Dorai, G. Wang, A.K. Jain, and C. Mercer, "Registration and Integration of Multiple Object Views for 3D Model Construction," *IEEE Trans. Pattern Analysis and Machine Intelligence,* vol. 20, no. 1, pp. 83-89, Jan. 1998.
[7] G. Blais and M.D. Levine, "Registering Multiview Range Data to Create 3D Computer Objects," *IEEE Trans. Pattern Analysis and Machine Intelligence,* vol. 17, no. 8, pp. 820-824, Aug. 1995.
[8] D. Huber and M. Hebert, "3D Modeling Using a Statistical Sensor Model and Stochastic Search," *Proc. IEEE Conf. Computer Vision and Pattern Recognition,* pp. 858-865, 2003.
[9] M. Reed and P. Allen, "3D Modeling from Range Imagery: An Incremental Method with a Planning Component," *Image and Vision Computing,* vol. 17, no. 2, pp. 99-111, 1999.
[10] A. Stoddart and A. Hilton, "Registration of Multiple Point Sets," *Proc. IEEE Int'l Conf. Pattern Recognition,* pp. 40-44, 1996.
[11] R. Bergevin, M. Soucy, H. Gagnon, and D. Laurendeau, "Towards a General Multi-View Registration Technique," *IEEE Trans. Pattern Analysis and Machine Intelligence,* vol. 18, no. 5, pp. 540-547, May 1996.
[12] G. Turk and M. Levoy, "Zippered Polygon Meshes from Range Images," *Proc. 21st Ann. Conf. Computer Graphics,* pp. 311-318, 1994.
[13] Y. Chen and G. Medioni, "Object Modeling by Registration of Multiple Range Images," *Image and Vision Computing,* vol. 10, no. 3, pp. 145-155, 1992.
[14] M. Rodrigues, R. Fisher, and Y. Liu, "Special Issue on Registration and Fusion of Range Images," *Computer Vision and Image Understanding,* vol. 87, nos. 1-3, pp. 1-7, 2002.
[15] A. Fitzgibbon, "Robust Registration of 2D and 3D Point Sets," *Proc. British Machine Vision Conf.,* pp. 662-670, 2001.
[16] A. Sappa, A. Restrepo-Specht, and M. Devy, "Range Image Registration by Using an Edge-Based Representation," *Proc. Int'l Symp. Intelligent Robotic Systems,* pp. 167-176, 2001.
[17] O. Faugeras and M. Hebert, "The Representation, Recognition, and Locating of 3D Objects," *Int'l J. Robotics Research,* vol. 5, no. 3, pp. 27-52, 1986.
[18] J. Wyngaerd and L. Van Gool, "Automatic Crude Patch Registration: Toward Automatic 3D Model Building," *Computer Vision and Image Understanding,* vol. 87, nos. 1-3, pp. 8-26, 2002.
[19] S. Yamany and A. Farag, "Free-Form Surface Registration Using Surface Signatures," *Proc. Int'l Conf. Computer Vision,* pp. 1098-1104, 1999.
[20] C. Chua and R. Jarvis, "3D Free-Form Surface Registration and Object Recognition," *Int'l J. Computer Vision,* vol. 17, no. 1, pp. 77-99, 1996.
[21] A. Johnson and M. Hebert, "Using Spin Images for Efficient Object Recognition in Cluttered 3D Scenes," *IEEE Trans. Pattern Analysis and Machine Intelligence,* vol. 21, no. 5, pp. 433-449, May 1999.
[22] C. Chen, Y. Hung, and J. Cheng, "RANSAC-Based DARCES: A New Approach to Fast Automatic Registration of Partially Overlapping Range Images," *IEEE Trans. Pattern Analysis and Machine Intelligence,* vol. 21, no. 11, pp. 1229-1234, Nov. 1999.
[23] P.J. Besl and N.D. McKay, "A Method for Registration of 3-D Shapes," *IEEE Trans. Pattern Analysis and Machine Intelligence,* vol. 14, no. 2, pp. 239-256, Feb. 1992.
[24] S. Rusinkiewicz and M. Levoy, "Efficient Variants of the ICP Algorithm," *Proc. Third Int'l Conf. 3-D Digital Imaging and Modeling,* vol. 1, pp. 145-152, 2001.
[25] G. Dalley and P. Flynn, "Pair-Wise Range Image Registration: A Study in Outlier Classification," *Computer Vision and Image Understanding,* vol. 87, no. 1, pp. 104-115, 2002.
[26] K.F. Man, K.S. Tang, and S. Kwong, "Genetic Algorithms: Concepts and Applications," *IEEE Trans. Industrial Electronics,* vol. 43, no. 5, pp. 519-534, 1996.
[27] S. Kirkpatrick, C. Gelatt, and M. Vecchi, "Optimization by Simulated Annealing," *Science,* vol. 220, no. 4598, pp. 671-680, 1983.
[28] D. Simon, M. Hebert, and T. Kanade, "Techniques for Fast and Accurate Intrasurgical Registration," *J. Image Guided Surgery,* vol. 1, no. 1, pp. 17-29, 1995.

[29] G. Champleboux, S. Lavallee, R. Szeliski, and L. Brunie, "From Accurate Range Imaging Sensor Calibration to Accurate Model-Based 3-D Object Localization," *Proc. IEEE Conf. Computer Vision and Pattern Recognition,* pp. 83-88, 1992.
[30] P. Chalermwat and T. El-Ghazawi, "Multi-Resolution Image Registration Using Genetics," *Proc. Sixth IEEE Int'l Conf. Image Processing,* vol. 2, pp. 452-456, 1999.
[31] M. Ahmed, S. Yamany, E. Hemayed, S. Ahmed, S. Roberts, and A. Farag, "3D Reconstruction of the Human Jaw from a Sequence of Images," *Proc. IEEE Conf. Computer Vision and Pattern Recognition,* pp. 646-653, 1997.
[32] K. Brunnstrom and A.J. Stoddart, "Genetic Algorithms for Free-Form Surface Matching," *Proc. 13th Int'l Conf. Pattern Recognition,* vol. 4, pp. 689-693, 1996.
[33] C. Robertson and R.B. Fisher, "Parallel Evolutionary Registration of Range Data," *Computer Vision and Image Understanding,* vol. 87, no. 1, pp. 39-50, 2002.
[34] S. Park and M. Subbarao, "A New Technique for Registration and Integration of Partial 3D Models," *Proc. SPIE Conf.,* vol. 4567, pp. 65-74, 2001.
[35] G. Dalley and P. Flynn, "Range Image Registration: A Software Platform and Empirical Evaluation," *Proc. Third Int'l Conf. 3-D Digital Imaging and Modeling,* vol. 1, pp. 246-253, 2001.
[36] Z.Y. Zhang, "Iterative Point Matching for Registration of Free-Form Curves and Surfaces," *Int'l J. Computer Vision,* vol. 13, no. 2, pp. 119-152, 1994.
[37] R. D'Agostino, *Tests for the Normal Distribution.* pp. 367-419, Marcel Dekker, 1986.
[38] J. Holland, *Adaptation in Natural and Artificial Systems.* Ann Arbor: The Univ. of Michigan Press, 1975.
[39] D.E. Goldberg, *Genetic Algorithms in Search, Optimization and Machine Learning.* Addison-Wesley Longman, 1989.
[40] P.H.S. Torr and A. Zisserman, "MLESAC: A New Robust Estimator with Application to Estimating Image Geometry," *Computer Vision and Image Understanding,* vol. 78, no. 1, pp. 138-156, 2000.
[41] P.F.U. Gotardo, O.R.P. Bellon, and L. Silva, "Range Image Segmentation by Surface Extraction Using an Improved Robust Estimator," *Proc. IEEE Conf. Computer Vision and Pattern Recognition,* 2003.
[42] P.F. U. Gotardo, O.R. P. Bellon, K.L. Boyer, and L. Silva, "Range Image Segmentation into Planar and Quadric Surfaces Using an Improved Robust Estimator and Genetic Algorithm," *IEEE Trans. Systems, Man, and Cybernetics, Part B,* 2004.
[43] J.M. Renders and S.P. Flasse, "Hybrid Methods Using Genetic Algorithms for Global Optimization," *IEEE Trans. Systems, Man, and Cybernetics Part B-Cybernetics,* vol. 26, no. 2, pp. 243-258, 1996.
[44] L. Ingber, "Very Fast Simulated Re-Annealing," *Math. Computer Modelling,* vol. 12, pp. 967-973, 1989.
[45] T. Masuda and N. Yokoya, "A Robust Method for Registration and Segmentation of Multiple Range Images," *Computer Vision and Image Understanding,* vol. 10, no. 3, pp. 295-307, 1995.

Luciano Silva received the BS and MSc degrees in informatics from the Universidade Federal do Paraná (UFPR), Brazil, in 1998 and 2000, respectively, and the PhD degree in electrical engineering and industrial informatics from the Centro Federal de Educação Tecnológica do Paraná (CEFET), Brazil, in 2003. In 2002-2003, he did his doctoral studies at the Signal Analysis and Machine Perception Laboratory at The Ohio State University. Since 2004, he has been with the Departmento de Informática of UFPR, where he is currently an assistant professor. He received the third place award in the undergraduate best paper contest and second place award in the master's thesis contest of the Brazilian Computer Society in 1998 and 2001, respectively. In 2004, he received the first place award in the doctoral dissertation contest of the XVII Brazilian Symposium on Computer and Image Processing (SIBGRAPI 2004), joint with II Ibero-American Symposium on Computer Graphics (SIACG 2004). His research interests include computer vision and graphics, image processing, and Linux operating systems. He is a member of the IEEE and the IEEE Computer Society.

Olga R.P. Bellon received the BS degree from the Universidade Federal do Espírito Santo (UFES), Brazil, in 1987, and the MSc and doctorate degrees from the Universidade Estadual de Campinas (UNICAMP), Brazil, in electrical engineering, in 1990 and 1997, respectively. In 1995, she founded the IMAGO Research Group in Computer Vision, Graphics, and Image Processing at the Departamento de Informática (DInf) of Universidade Federal do Paraná (UFPR), where she is an associate professor. From 1997-2000, she was the head of the Graduate Program of Informatics, DInf. From 2000 to 2002, she was the general research coordinator at UFPR. She spent a sabbatical year as a visiting scholar in the Signal Analysis and Machine Perception Laboratory in the Department of Electrical and Computer Engineering at The Ohio State University. She was the general chair of the XVII Brazilian Symposium on Computer and Image Processing (SIBGRAPI 2004), joint with II Ibero-American Symposium on Computer Graphics (SIACG 2004). Her main research interests lie in range image segmentation and registration, digital archaeology, virtual museum, image mining, medical imaging, segmentation and classification of high resolution satellite images, and accessibility tools for people with low vision and special needs. She is a member of the IEEE and the IEEE Computer Society.

Kim L Boyer received the BSEE (with distinction), MSEE, and PhD degrees, all in electrical engineering, from Purdue University in 1976, 1977, and 1986, respectively. From 1977 through 1981, he was with Bell Laboratories, Holmdel, New Jersey; from 1981 through 1983 he was with Comsat Laboratories, Clarksburg, Maryland. Since 1986, he has been with the Department of Electrical and Computer Engineering, The Ohio State University, where he holds the rank of professor. In 1986, he founded the Signal Analysis and Machine Perception Laboratory at Ohio State. He is a fellow of the IEEE and a fellow of the IAPR. He is a former IEEE Computer Society Distinguished Speaker. Dr. Boyer's research interests include all aspects of computer vision and medical image analysis, including perceptual organization, structural analysis, graph theoretical methods, stereopsis in weakly constrained environments, optimal feature extraction, large model bases, and robust methods. He is a past Scientific Secretary of Commission III (Theory and Algorithms) of the International Society for Photogrammetry and Remote Sensing, a former associate editor of the *IEEE Transactions on Pattern Analysis and Machine Intelligence*, an area editor of *Computer Vision and Image Understanding*, associate editor of *Machine Vision and Applications*, a former associate editor of *Pattern Recognition*, cogeneral chair of the first two IEEE Computer Society Workshops on Perceptual Organization, a charter member of the DARPA IUE Technical Advisory Committee, and a member of the initial ORD RADIUS Technical Oversight Committee. In 1993, with Kuntal Sengupta, he won the Siemens Best Paper Award at the IEEE Computer Society Conference on Computer Vision and Pattern Recognition. In 1995, a student team codirected by Professor Boyer won the International Unmanned Ground Vehicle Competition for its vision-guided autonomous robotic transporter. In 2002, he was the program cochair for computer vision and robotics at the International Conference on Pattern Recognition, Quebec. He is a member of the governing board for the International Association for Pattern Recognition and chair of the IEEE Computer Society Technical Committee on Pattern Analysis and Machine Intelligence. He was the keynote speaker for this year's SIBGRAPI Conference in Curitiba, Brazil. Dr. Boyer has published four books: *Computing Perceptual Organization in Computer Vision* (World Scientific, 1994 (with Sudeep Sarkar)); *Applications of AI, Machine Vision, and Robotics* (World Scientific, 1994 (with Louise Stark and Horst Bunke, eds.)); *Perceptual Organization for Artificial Vision Systems* (Kluwer Academic, 2000 (with Sudeep Sarkar, eds.)); and *Robust Range Image Registration Using Genetic Algorithms and The Surface Interpenetration Measure* (World Scientific, in press (with L. Silva and O.R.P. Bellon)).